Kobayashi S, Kaneko Y, Seino K, Yamada Y, Motohashi S, Koike J, Sugaya K, Kuriyama T, Asano S, Tsuda T, Wakao H, Harada M, Kojo S, Nakayama T., Taniguchi M	Impaired IFN-γ production of Vα24 NKT cells in non-remitting sarcoidosis	Int. Immunol.	16	215-222	2004
Harada M, Seino K, Wakao H, Sakata S, Ishizuka Y., Ito T, Kojo S, Nakayamat, Taniguchi M	Down-regulation of the invariant Vα14 antigen receptor in NKT cells upon activation	Int. Immunol.	16	241-247	2004
Hiroshima K, Iyoda A, Shibuya K, Haga Y, Toyozaki T, Iizawa T, Nakayama T, Fujisawa T, Ohwada H	Genetic alterations in an early-stage pulmonary large cell neuroendocrine carcinoma	Cancer	100	1190-1198	2004
Kondo N, Ishii Y, Son A, Sakakura-Nishiyama J, Kwon Y W, Tanito M, Nishinaka Y, Matsuo Y, Nakayama T, Taniguchi M, Yodoi, J	Cysteine-dependent immune regulation by TRX and MIF/GIF family proteins	Immunol. Letters	92	143-147	2004
Inami M, Yamashita M, Tenda Y, Hasegawa A, Kimura M, Hashimoto K, Seki N, Taniguchi M, Nakayama T	CD28 costimulation controls histone hyper-acetylation of the IL-5 gene locus in developing Th2 cells	J. Biol. Chem.	279	23123-133	2004
Yamashita M, Miyamoto T, Ukai-Tadenuma M, Sugaya K, Hosokawa H, Hasegawa A, Kimura M, Taniguchi M, DeGregori J, Nakayama T	Essential role of GATA3 for the maintenance of type2 helper T (Th2) cytokine production and chromatin remodeling at the Th2 cytokine gene loci	J. Biol. Chem.	279	26983-990	2004
Shimizu E, Koike J, Wakao H, Seino K, Koseki H, Kakiuchi T, Nakayama T, Taniguchi M.	Role of a NK receptor , KLRE-1, in bone marrow allograft rejection: analysis with KLRE-1 deficient mice	Blood	104	781-783	2004
Yamashita M, Shinnakasu R, Nigo Y, Kimura M, Hasegawa A, Taniguchi M, Nakayama T	Interleukin (IL)-4-independent maintenance of histone modification of the IL-4 gene loci in memory Th2 cells	J. Biol. Chem.	279	39454-464	2004
Nakai Y, Iwabuchi K, Fujii S, Ishimori N, Dashtsoodol N, Watano K, Mishima T, Iwabuchi C, Tanaka S, Bezbradica J S, Nakayama T, Taniguchi M, Miyake S, Yamamura T, Kitabatake A, Joyce S, Van Kaer L, Onoe K	Natural killer T cells accelerate atherogenesis in mice. Short title: NKT cells and atherosclerosis in mice	Blood	104	2051-2059	2004
Diano H, Kon S, Iwabuchi K, kimura C, Morimoto J, Ito D, Segawa T, Maeda M, Hamuro J, Nakayama T, Taniguchi M, Ygaita H, Van kaer L, Onoe K, Uede T Denhardt D, Rittling S,	Osteopontin as a mediator of NKT cell function in T cell-mediated liver diseases	Immunity	21	539-550	2004

Katsumoto T, Kimura M, Yamashita M, Hosokawa H, Hashimoto K, Hasegawa A, Omori M, Miyamoto T, Taniguchi M, Nakayama T	STAT6-dependent differentiation and production of IL-5 and IL-13 in murine NK2 cells	J. Immunol.	173	4967-4975	2004
Kimura M, Hosokawa H, Yamashita M, Watarai H, Hasegawa A, Iwamura C, Taniguchi M, Takagi T, Ishii S, Nakayama T.	Regulation of Th2 cell differentiation by murine Schnurri-2	J. Exp. Med.		in press	2005
Ishikawa A, Motohashi S, Ishikawa E, Fuchida H, Higashino K, Otsuji M, Iizawa T, Nakayama T, Taniguchi M, Fujisawa T	A phase I study αgalactosylceramide (KRN7000)-pulsed dendritic cells in patients with advanced and recurrent non-small cell lung cancer	Clin. Can. Res.		in press	2005
山下政克、中山俊憲	BCGによるI型アレルギー疾患治療の可能性	医学のあゆみ	208(3)	171-176	2004
中山俊憲、清野宏、笹月健彦	免疫研究分野のフロンティア:分子、細胞から個体レベルでの免疫システムの解明とそれが導く新しい臨床応用	実験医学増刊			2004
中山俊憲	システムとしての免疫系ー分子、細胞、場のダイナミックな統合とシステムの破綻としての免疫疾患	実験医学増刊	22(5)	16-20	2004
山下政克、中山俊憲	Th2/Tc2細胞分化に伴うTh2サイトカイン遺伝子(IL-4、IL-5、IL-13)座のクロマチンリモデリング	実験医学増刊	22(5)	64-71	2004
本橋新一郎、中山俊憲	NKT細胞免疫系活性化によるがん免疫療法	Medical Science Digest	30(4)	29-33	2004
木村元子、中山俊憲	アレルギー疾患とヘルパーT細胞の機能	アレルギー・免疫別冊	11(4)	32-39	2004
山下政克、中山俊憲	クロマチン修飾を介した免疫反応の制御:Th2細胞分化をモデルに	細胞工学	23(10)	1166-1170	2004
中山俊憲	Th1/Th2細胞免疫システムの形成と維持ーTh2-依存性の気道炎症制御機構とTh2サイトカイン遺伝子(IL-4、IL-5、IL-13)座のクロマチンリモデリングー	耳鼻免疫アレルギー	22(3)	001-008	2004
山下政克、中山俊憲	Th2細胞分化に伴うTh2サイトカイン遺伝子座のクロマチンリモデリング	Molecular Medicine 免疫2005	41	011-019	2004
中山俊憲	アレルギー発症を制御するTh2細胞の分化・機能維持に関する研究	アレルギア	33	88-92	2004
Kudo N, Yasumasu S, Iuchi I, Tanokura M	Crystallization and prelimimary X-ray analysis of HCE-1, a hatching enzyme of Medaka fish, *Oryzias latipes*	Acta Crystal.	D60	725-726	2004
Kim Y T, Kurita R, Kojima M, Nishii W, Tanokura M, Muramatsu T, Ito H, Takahashi K	Identification of arginine residues important for the activity of *Escherichia coli* signal peptidase	I. Biol. Chem.	385	381-388	2004
Nara M, Yumoto F, Nagata K, Tanokura M, Kagi H, Ojima T, Nishita K	Fourier transform infrared spectroscopic study on the binding of Mg2+ to a mutant Akazara scallop troponin C (E142Q)	Biopolymers	74	77-81	2004
Miyazono K, Kudo N, Tanokura M	Cloning, purification, crystallization, and preliminary crystallographic analysis of acylphosphatase from *Pyrococcus horikoshii* OT3	Acta Crystal.	D60	1135-1136	2004
Kamo M, Kudo N, Lee W C, Motoshima H, Tanokura M	Crystallization and prelimimary X-ray crystallographic analysis of peptide deformlase from *Thermus thermophilus* HB8	Acta Crystal.	D60	1299-1300	2004

Kato Y, Nagata K, Lian L, Takahashi M, Herrero J, Sudol M, Tanokura M	Common mechanism of ligand recognition by group-Ⅱ/ⅢWW domains - Refinding their functional classification	J. Biol. Chem.	279	31833-841	2004
Bekker E G, Creagh A L, Sanaie N, Yumoto F Y, Lau G H, Tanokura M, Haynes C A, Murphy MEP	Specificity of the synergistic anion for iron-binding by ferric binding protein from *Neisseria gonorrhoeae*	Biochemistry	43	9195-9203	2004
Hu F, Furihata K, Ito-Ishida M, Kaminogawa S, Tanokura M	Nondestructive observation of bovine milk by NMR spectroscopy: Analysis of existing states of compounds and detection of new compounds	J. Agr. Food Chem.	52	4969-4974	2004
Nagata K, Tsutsui S, Lee W C, Ito K, Kamo M, Inoue Y, Tanokura M	Crystallization and preliminary X-ray analysis of carboxypeptidase 1 from *Thermus thermophilus*	Acta Crystal.	D60	1445-1446	2004
Kato Y, Akai A, Suzuki R, Hosokawa H, Ninomiya H, Masaki T, Nagata K, Tanokura M	1H, 13C and 15N assignments of the tandem WW domains of human MAGI-1/BAP-1	J. Biomol. NMR	29	539-540	2004
Lee W C, Ohshiro T, Matsubara T, Izumi Y, Tanokura M	Crystallization and preliminary X-ray analysis of desufurization enzyme DszB and its C27S mutant complexed with biphenyl-2-sulfinic acid	Acta Crystal.	D60	1636-1638	2004
Oda Y, Muramatsu T, Ito M, Yumoto F, Tanokura M	Backbone 1H, 13C and 15N resonance assignment of the N-terminal domain of human eRF1	J. Biomol. NMR	30	109-110	2004
Furusawa Y, Nagarajan V, Tanokura M, Masai E, Fukuda M, Senda T	Crystal structure of the terminal oxygenase component of biphenyl dioxygenase derived from *Rhodococcus* sp. Strain RHA1	J. Mol. Biol.	342	1041-1052	2004
Sasaki H, Nakagawa A, Muramatsu T, Suganuma M, Sawano Y, Kojima M, Kubota K, Takahashi K, Tanokura M	The three dimensional structure of aspergilloglutamic peptidase from *Aspergillus niger*	Proc. Japan Acad.	80B	435-438	2004
Miyazono K, Sawano Y, Tanokura M	Crystal structure of acylphosphatase from hyperthemophilic archaeon *Pyrococcus horikoshii* OT3	Proc. Japan Acad.	80B	439-442	2004
Pan D, Tanokura M	Purification and characterization of an aminopeptidase from *Lactobacillus helveticus* JCM1004	Food Chem.	88	511-516	2004
Suzuki T, Someya S, Hu F, Tanokura M	Comparative study of catechin composition in five Japanese perisimmons (*Diospyros kaki*)	Food Chem.		in press	2005
加藤有介、田之倉優	リン酸化とタンパク質立体構造	Molecular Medicine	41	522-529	2004
田之倉優、李愚哲	タンパク質の結晶化とX線構造解析ーニトロ／フラビン還元酵素と脱硫酵素を例として	日本農芸化学会誌	78	565-567	2004
加茂昌之、田之倉優	タンパク質の形をみた立役者たち. X線結晶構造解析による高精度立体構造解析	化学と教育	52	463-466	2004
岩崎わかな、田之倉優	EF-hand 蛋白質CBP40のカルシウム結合および非結合状態の立体構造	日本結晶学会誌	46	359-363	2004
Muramatsu T, Oda Y, Yumoto F, Ito M, Tanokura M	Analysis of dynamic structure of eukaryotic release factor 1 (eRF1)	Bioimages	12	37-37	2004
Furusawa K, Matsumura H	Colloidal nanoparticles: Electrokinetic characterization	Dekker Encyclopedia of Nanoscience and Nano technology		773-786	2004
Matsumura H., Neytchev V., Terezova N., Tsoneva I.	Ca ion permeation through liposome membranes with heat generation by square-wave electric field	Colloids and Surfaces B: Biointerfaces	33	243-249	2004

Hoshino A, Fujioka K, Oku T, Suga M, Yu F, Sasaki F, Ohta T, Yasuhara M, Suzuki K, Ymamoto K	Physico-chemical properties and cellular toxicity of nanocrystal quantum dots depend on their surface modification	Nano Letters		in press	2005
Yamamoto K, Manabe N	Randomnes and organization of the bio-nano-particles into the functional structure	Theoretical and Applied Mechanics, Japan	53	111-114	2004
Aringazin A.K., Dahnovsky Y., Krevchik V.D., Semenov M.B., Ovchinnikov A.A., Yamamoto K.	Two-dimensional tunnel bifurcations with dissipation	Hadronic Journal	27(N2)	115-150	2004
Himeda T, Ohara Y, Asakura K, Kontani Y, Murakami M, Suzuki H, Sawada M	A lentiviral expression system demonstrates that L(*) protein of Theiler's murine encepha-lomyelitis virus (TMEV) is essential for virus growth in a murine macrophage-like cell line	Virus Res	108	23-28	2005
Imamura K, Hishikawa N, Ono K, Suzuki H, Sawada M Nagatsu T, Yoshida M, Hashizume Y	Cytokine production of activated microglia and decrease in neurotrophic factors of neurons in the hippocampus of Lewy body disease brains	Acta Neuropathol.		in press	2004
鈴木弘美、澤田誠	脳機能障害とミクログリアのかかわりおよび細胞を用いた標的化治療・診断	医学のあゆみ	210(3)	187-190	2004
塚田孝祐	低酸素のバイオイメージング	医学のあゆみ「レドックス」		in press	2005
Higashi K, Takasawa R, Yoshimori A, Goh T, Tanuma S, Kuchitsu K	Identification of a novel gene family, paralogs of an inhibitor of apoptosis proteins present in plants, fungi, and animals	Apoptosis		in press	2005
Fukuta N, Miyasaka M, Saitou R, Kuchitsu K	The relationship between various image of acyanic petal of Eustoma gradifrorum under UV light and flavonoid conmtent	Hort. Res.		in press	2005
Kadota Y, atanabe T, Fujii S Maeda Y, Ohno R, Higashi K Sano T, Muto S, Hasezawa S, Kuchitsu K	Cell-cycle dependence of elicitor-induced signal transduction in tabacco BY-2 cells	Plant Cell Physiol.	46(1)	156-165	2005
Karita E, Yamakawa H, Mitsuhara I, Kuchitsu K, Ohashi Y	Three types of tabacco calmodulins chara-cteritically activate plant NAD kinase at different Ca2+ concentration and pHs	Plant Cell Physiol.	45(11)	1371-1379	2004
Kadota Y, Watanabe T, Fujii S, Higashi K, Sano T, Nagata T, Hasezawa S, Kuchitsu K	Crosstalk between elicitor-induced cell death and cell cycle regulation in tabacco BY-2 cells	The Plant J.	40(10)	131-142	2004
Kurusu T, Sakurai S, Miyao A, Hirochika H, Kuchitsu K	Identification of a putative voltage-gated Ca2+ permeable channel (OsTPC1) involved in Ca2+ influx and regulation of growth and development in rice	Plant Cell Physiol.	45(6)	693-702	2004
Kadota Y, Furuichi T, Ogasawara Y, Goh T, Higashi K, Muto S, Kuchitsu K	Identification of a putative voltage-dependent Ca2+ permeable channel involved in cryptogein-induced Ca2+ transients and defense responses in tobacco BY-2 cells	Biochem. Biophys. Res. Comm.	317	823-830	2004
Kadota Y., Goh T., Tomatsu H., Tamauchi R., Higashi K., Muto S., Kuchitsu K.	Cryptogein-induced initial events in tobacco BY-2 cells: Pharmacological characterization of molecular relation-ship among cytosolic Ca2+ transients anion efflux and production of reactive oxygen species	Plant Cell Physiol.	45(2)	160-170	2004

Kuriyama I., Asano N., Kato I., Oshige M., Sugino A., Kadota Y., Kuchitsu K., Yoshida H., Sakaguchi K., Mizushina Y.	L-Homoserylaminoethanol, a novel dipeptide alcohol inhibitor of eukaryotic DNA polymerase E from a plant cultured cells, *Nicotina tabacum* L.	Bioorganic & Medicinal Chemistry	12	957-962	2004
朽津和幸	植物がストレスを感じる仕組みを「見る」ーホルモン受容部位や情報の伝達を可視化するバイオイメージング技術の開発	バイオデザインー生物の形と機能ー、NIASアグリバイオサイエンスシリーズ	1	60-62	2004

Role of Oxidative Stress in Interaction Between Endothelial Cells and Platelets in Diabetes

YASUNORI HIROSE[1], EIICHI SEKIZUKA[3], HIROMICHI NAKADATE[1], TADASHI OZAWA[1], HARUYUKI MINAMITANI[1], CHIKARA OSHIO[4], and HIROMASA ISHII[2]

Key words. Diabetes mellitus, Endothelial cell, Platelet, Advanced glycation end product, Oxidative stress

Introduction

Diabetes mellitus is characteristic of chronic hyperglycemia, and causes various angiopathies. The population of diabetic patients continues to increase, so it is important to clarify the mechanisms of angiopathies and to apply the results to treatment strategies.

The disorders of the circulating system in diabetes mellitus are categorized into macroangiopathy, coronary heart disease, cerebral infarction or arteriosclerosis, and microangiopathy, nephropathy, retinopathy, and neuropathy. Among major factors reported are decreased erythrocyte deformability [1], increased leukocyte chemotaxis, abnormal platelet adherence and aggregation [2], and increased plasma viscosity. However, the mechanisms of these dysfunctions are not clarified as yet, especially in microangiopathy.

In previous studies, we investigated thrombus formation in the mesenteric arterioles of diabetic rats using a photochemical reaction. We confirmed that there was a shortening of thrombus formation times in diabetic rats, but we are unable to clarify the main contributors to thrombus formation in diabetes

[1]Graduate School of Science and Technology, Keio University, 14-1 Hiyoshi 3-chome, Kohoku-ku, Yokohama, Kanagawa 223-0061, Japan
[2]Department of Internal Medicine, Keio University School of Medicine, 35 Shinanomachi, Shinjuku-ku, Tokyo 160-8582, Japan
[3]Department of Clinical Research, National Saitama Hospital, 2-1 Suwa, Wako, Saitama 351-0102, Japan
[4]Oshio Clinic, 2-6-2 Kanda Awajicho, Chiyoda-ku, Tokyo 101-0063, Japan

mellitus, platelets or endothelial cells (ECs). Furthermore, it has been suggested in recent studies that radical oxygen levels rise in diabetic conditions and injure the vessels, leading to some complications. Therefore, we herein investigate the interaction of platelets and ECs under diabetic conditions and the contribution of radical oxygen species (ROS).

Material and Methods

Human umbilical vein ECs were cultured in high D-glucose or N-epsilon-(carboxymethyl)lysine-modified advanced glycation end-products (CML-AGE) in culture solution to assume diabetic conditions. Endothelial cells were kept in culture until they became confluent. We used human healthy platelets and diabetic platelets (HbA1c > 6.5). Blood was drawn from healthy or diabetic donors and mixed with 3.8% sodium citrate at a ratio of 9:1 and centrifuged at 100×*g* for 10 min to make platelet-rich plasma. Platelet-rich plasma was diluted with self-plasma to adjust platelet concentration to 300 000/μl.

After culturing ECs in various conditions, Photofrin as the photosensitizer was added to the culture solution and incubated for 30 min. Platelet-rich plasma was brought into contact with incubated ECs, and we irradiated the excitation light and damaged ECs. After light irradiation, we measured the platelet adhesion area (PAA) on ECs by NIH imaging.

To study the effect of ROS for platelet adhesion to ECs, we incubated superoxide dismutase (SOD), catalase, or dimethyl sulfoxide with high D-glucose or high CML-AGE. In this case, we did not use the photochemical reaction in order to eliminate the influence of ROS generated by photochemical reaction. Platelet-rich plasma was brought into contact with ECs for 30 min without photochemical reaction. The method used to calculate PAA was the same as described above.

Results

Platelet adhesion area changed according to the diabetic conditions. When ECs were cultured with high glucose or high CML-AGE, PAA increased significantly compared to normal culture conditions. Platelet adhesion area in diabetic platelets was not different to that from normal platelets under any condition.

Platelet adhesion area was reduced by ROS scavengers in high glucose or high AGE. Radical oxygen species scavengers reduced the increase of PAA by high glucose or high AGE, but did not restore it to the normal level. Suppression of platelet adhesion by H_2O_2 and $^{\cdot}OH$ scavenger was stronger in high CML-AGE than in high D-glucose.

Discussion

Platelet adhesion area increases with diabetic ECs but not with diabetic platelets. So it can be said that ECs under diabetic conditions contributed much more to platelet adhesion than diabetic platelets. This suggests that easy thrombus formation in diabetes mellitus is mainly caused by the dysfunction of ECs.

Platelet adhesion area reduction ratios by various ROS scavengers were calculated based on increased PAA in high glucose or high CML-AGE. The result indicates that the damage of ECs by H_2O_2 and $^{\cdot}OH$ is heavier in high AGE than in high glucose.

Reactive oxygen species is the major cause of injury to ECs, which leads to platelet adhesion in high glucose and high CML-AGE. Other factors still remain to be considered regarding endothelial damage in diabetic conditions.

Conclusion

Enhanced thrombogenesis in diabetes mellitus is mainly caused by endothelial injury due to excess ROS production induced by chronic hyperglycemia and AGEs subsequent to it.

References

1. Tsukada K, Sekizuka E, Oshio C, et al. (2001) Direct measurement of erythrocyte deformability in diabetes mellitus with a transparent microchannel capillary model and high-speed video camera system. Microvasc Res 61(3):231–239
2. Ozawa T, Sekizuka E, Oshio C, et al (2002) Mechanism of increased platelet aggregation in diabetes mellitus—newly-devised investigation with laser scattering platelet aggregometer. Microcirc Annu 18:53–54

臓器血流と酸素代謝の光・イメージング解析

Photonic imaging analysis of blood flow and oxygen tension in organ microcirculation

南谷晴之(写真)　塚田孝祐

Haruyuki MINAMITANI[1] and Kousuke TSUKADA[2]

慶應義塾大学理工学部物理情報工学科[1]，同医学部医化学教室[2]

◎脳，肝などの実質臓器の微小循環や腫瘍新生血管の血流動態を可視化するとともに，臓器内のミクロレベルでの酸素代謝を同時計測し，組織や細胞の機能変化を解析することはフィジオーム研究の一重要課題となっている．組織や細胞を傷めることなく非接触で計測するには，螢光やリン光を発する分子プローブを細胞に標識し，特定波長の光で励起して螢光イメージやリン光信号を検出する方法が有効である．著者らは多波長励起の光・イメージング解析システムを開発し，FITC 螢光色素で選択的に赤血球を標識し，励起波長 450 nm，螢光波長 520 nm で可視化することで脳虚血に伴う微小循環血流変化を定量解析した．また，酸素感受性色素 Pd ポルフィリンをラット大腿静脈から投与し，波長 532 nm のパルスレーザーで励起し，発光リン光 700 nm をフォトマルで検出して，酸素 quenching 作用によるリン光寿命の変化から微小血管内の酸素分圧を計測することに成功した．

Key word：微小循環，臓器血流，酸素分圧，バイオイメージング，螢光・リン光

臓器微小循環とバイオイメージング

血液は心ポンプの働きで全身に行き渡り，組織に酸素や栄養素を運び，引き換えに二酸化炭素や老廃物を受け取り，組織から排出する役割を担っている．このようなガス交換や物質代謝が行われる領域は，非常に細い細動脈，細静脈，毛細血管，微小リンパ管などの微小循環で構成されており，生命現象の恒常性維持にもっとも重要な役割を果たしている．

近年，増大傾向にある成人病疾患にかかわる脳，腎，肝など各種臓器の微小循環内の血流動態を可視化し，循環機能と疾患との因果関係や薬理効果を詳細に検討する必要性が高まっている．また，循環不全とのかかわりにおいて臓器内のミクロなレベルでの酸素代謝を同時計測し，組織や細胞の機能変化を観測することも重要な課題となっている．一方，ナノテクノロジーは，超微細なレベルで原子・分子を操作したり微小な粒子や機械を作製する技術であるが，バイオ・医療技術と組み合わせたり光・イメージング技術との融合により，生体の分子・オルガネラ・細胞レベルの構造や機能を詳細に解析することを可能としている．

微小循環系の血流や酸素代謝を計測し，定量解析する方法については多くの研究があるが，本稿ではナノプローブとバイオイメージング技術を利用した臓器血流と酸素代謝の光・イメージング解析法を紹介し，虚血脳組織および腫瘍組織の微小循環血流と酸素分圧計測の結果について述べる．

臓器微小循環の光・イメージング解析システム

微小循環研究では対象動物の実質臓器を顕微鏡下に展開し，目標となる細胞・オルガネラなどの形態・動態を可視化することが重要である．その際，フルオロフォア分子，ポルフィリン化合物，螢光蛋白などのナノプローブを生体中に局所投与

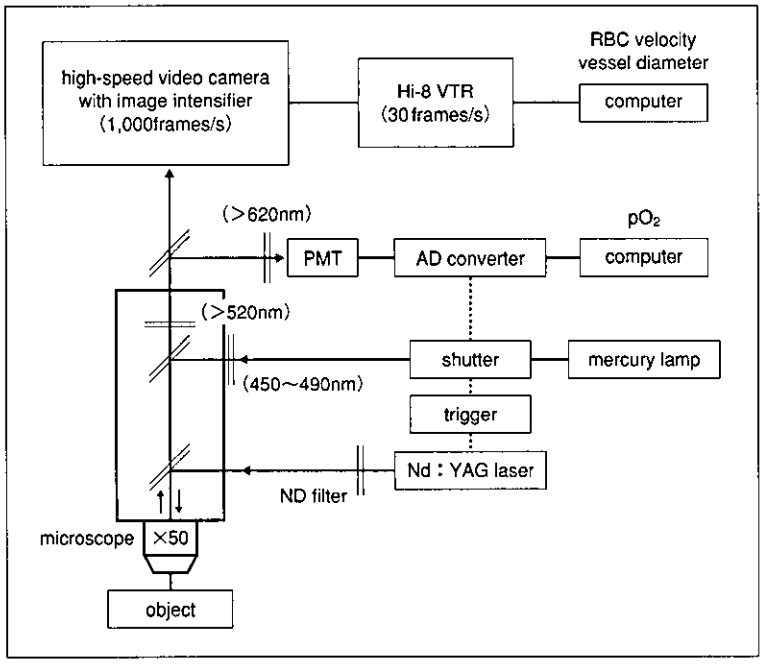

図 1　臓器微小循環の血流と酸素分圧を同時計測する光・イメージング解析システム

し，脳・肝・腎などの臓器微小循環における血流・酸素代謝機能や腫瘍，糖尿病，血栓症などの病態における微小循環障害を分子・細胞レベルでイメージング解析して，障害・再生・治癒機構を解明することが多い．生体分子やオルガネラと結合したナノプローブを使うことにより，超微細な一分子イメージングやイオン種イメージングが可能となるが，超高速度高感度カメラ，高速走査型共焦点レーザー顕微鏡などのイメージングシステムが利用される[1]．

著者らは，顕微鏡下で透過光観測が不可能な厚みを有する臓器において，蛍光プローブを用いた血流可視化と酸素電極を用いることなく，リン光プローブによる血中酸素分圧の同時計測法を開発した[2-4]．血流速度計測システムは，顕微鏡に接続された高速度高感度ビデオカメラ，汎用 Hi8 ビデオレコーダ，画像処理ボードを実装したビデオ制御・画像解析コンピュータ，画像相関法・流速解析ソフトなどで構成される．実質臓器や組織内の微小血管の血行動態は，FITC-dextran(励起波長 488 nm，蛍光波長 520 nm)20 mg/ml を iv 投与し，血漿成分の流動現象を可視化して全血血流動態の定量化を行うことができる．また，あらかじめ循環赤血球の約 5% を採血し，これを体外で蛍光プローブ FITC(励起波長 488 nm，蛍光波長 520 nm)で *ex vivo* 標識した後，返血し，顕微鏡下で微小血管を流れる個々の蛍光標識赤血球の流動現象を可視化することによって赤血球の流速計測が可能となる．白血球の可視化には，アクリジンオレンジ(励起波長 430 nm，蛍光波長 530 nm)0.5 mg/kg を iv 投与し体内染色するか，ローダミン 6G(励起波長 514 nm，蛍光波長 590 nm)50 μg/ml で *ex vivo* 標識して微小血管内の白血球のローリングや粘着数を可視化計測する．血小板の可視化には CFSE(励起波長 494 nm，蛍光波長 520 nm)かローダミン 6G を iv 投与・体内染色するか，CFDASE(励起波長 492 nm，蛍光波長 517 nm)で *ex vivo* 標識して微小血管内の流動，血小板血栓生成動態を可視化評価する．

一方，酸素電極を組織・血管中に刺入することなく非接触・無侵襲に血中酸素分圧を計測するために，リン光発光・酸素プローブ Pd ポルフィリン〔Pd-meso-tetra-(4-carboxyphenyl)-porphyrin：Pd-TCPP〕を用い，光励起後のリン光寿命より酸

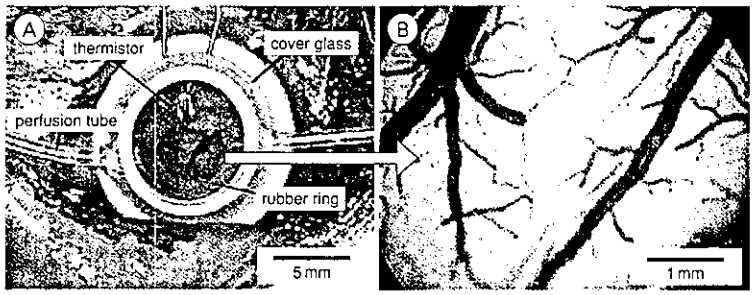

図 2　ラット脳表層の微小循環血流と酸素代謝を観測するための closed cranial window(A)と，微小循環系の血管構築(B)

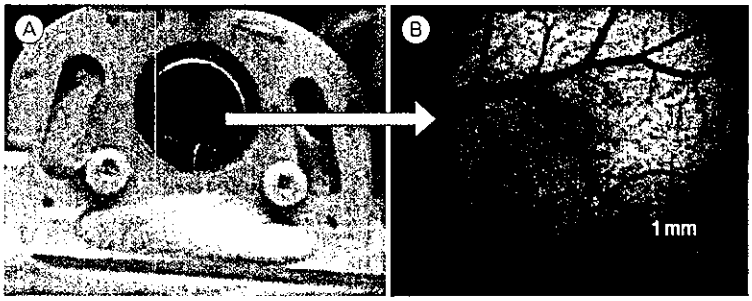

図 3　マウス背部皮膚層の微小循環血流と酸素代謝を観測するための dorsal skinfold chamber(A)と，皮膚層に移植した腫瘍組織と腫瘍新生血管(B)

素分圧を計測する技術を開発した．あらかじめ，対象動物に Pd ポルフィリンを iv 投与し，対象となる微小血管に励起パルス光(Nd：YAG laser SH，波長 532 nm)を照射する．酸素濃度に依存して発光するリン光を 620 nm のロングパスフィルタを介してフォトマルで光電変換し，AD 変換後にパソコンで波形処理してリン光寿命 τ より，つぎの Stern-Volmer 式に基づいて酸素分圧 pO_2 を求める．

$$\tau_0/\tau = 1 + K\tau_0 pO_2$$

ここで τ_0，τ はそれぞれ酸素分圧が 0 および pO_2mmHg のときのリン光寿命，K は Stern-Volmer 定数であるが，上式からわかるように酸素分圧が高まるとリン光強度は低下，寿命は短縮する．図 1 に示す蛍光・リン光ナノプローブを用いたマルチフォトニック・イメージングシステムは著者らによって実用化されており，臓器微小血管内の血流速度・酸素分圧の同時計測だけでなく，異なる波長の光源と受光・受像系を加えることにより，*in vivo* 実験系で多種類の細胞・組織の分子生理機能を解析することができる．

図 2 は，脳表層の微小循環血流と酸素代謝を観測するためのラット頭頂部に設置した closed cranial window と，window 内で観測された細動脈，細静脈，毛細血管などの微小循環系の血管網を示したものである．図 3 はマウス背部皮膚層の微小循環血流と酸素代謝を観測するための dorsal skinfold chamber と，chamber 内で観測された腫瘍組織と腫瘍新生血管網を示したものである．後者は，乳癌細胞 MT060562 を埋め込み増殖させ，それに伴って構築された新生血管である．このような特殊な装置を使い，小動物の対象領域の微小循環血流動態を種々の病態や条件下で慢性的あるいは急性的に観測しイメージング解析することが可能である．

臓臓器血流と酸素代謝の光・イメージング解析

図 4 は closed cranial window 内の Wistar 系雄性ラット脳表層の細動脈と，細静脈を流れる FITC

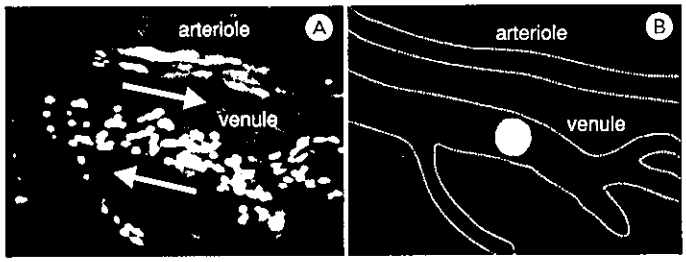

図 4　ラット脳表層の細動脈と細静脈を流れる FITC 標識赤血球(A)と，血中酸素分圧を計測するためのレーザー光スポット(B)

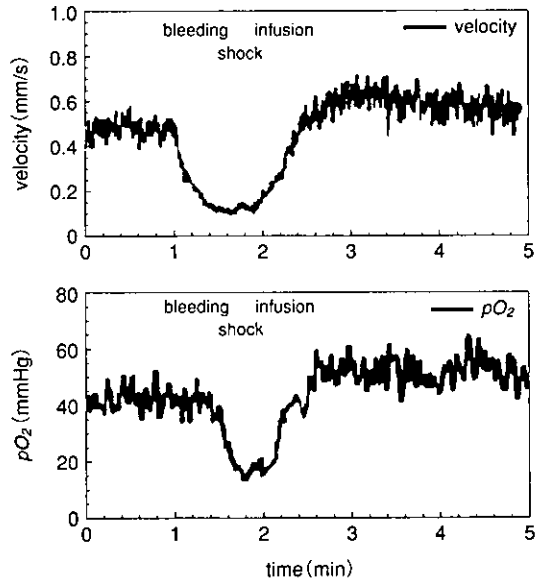

図 5　ラット脳表層細静脈内(図 4)の赤血球流速と血中酸素分圧の時間経過

3 ml の脱血ショックと 1 分後の返血再灌流を施行.

図 6　光化学反応による活性酸素産生に基づく脳表層微小血管内の血小板血栓形成

標識赤血球であり，図 4-B の中央の白いスポットは直径約 30 μm の Nd：YAG パルスレーザー(第 2 高調波：532 nm)の照射部位である．この位置を流れる血液中の Pd-TCPP がレーザー励起されてリン光を発するが，放射されるリン光強度と寿命は酸素濃度によって変化する．実験には Pd-TCPP 生食水溶液(10 mg/ml)を静脈投与し，事前に求めておいた酸素分圧とリン光寿命の校正曲線に基づき，臓器微小血管内の酸素分圧を計測した．本計測システムでは Nd：YAG レーザー第 2 高調波パルス光の繰返し周波数信号(1 Hz)をトリガーとして電子シャッターを駆動し，FITC 標識赤血球の励起光と Pd-TCPP への励起光を交互に照射し，そのタイミングに合わせて蛍光血流収録画像とフォトマルで検出したリン光信号をコンピュータ解析した．

図 5 は観測結果を示したもので，図 4 のラット脳表層細静脈内の赤血球流速と血中酸素分圧の時間経過である．3 ml の脱血による急性出血ショックを起こさせたとき，微小循環血流速度および酸素分圧の急激な低下がみられ，1 分後に返血再灌流を施行したところ，双方とも回復するが，前値を上回った後にしだいに前値に収束する傾向が認められた．ラットの肝類洞血管においても急性出血ショックおよび辺血蘇生時の血流動態と酸素分圧を同時計測した結果，臓器特異性があるものの同様な結果が得られ，実質臓器内の虚血，出血性ショックおよび血液再灌流時の微小循環機能の変化を精度よくとらえることができた．

図 6 は光化学反応による活性酸素産生に基づく脳表層微小血管内の血小板血栓形成を示したものであり，脳組織は梗塞により局所的に虚血状態となる．血小板はローダミン 6G を iv 投与して体内

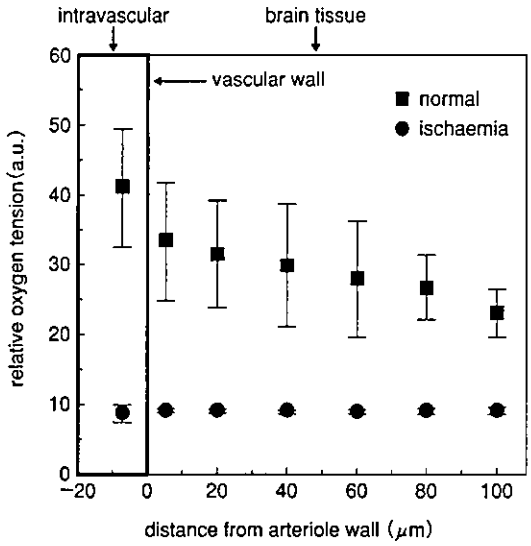

図 7　ラット脳細動脈および周辺脳組織内の血中酸素分圧の空間分布
光化学反応血栓形成法で梗塞した血管と周辺組織では著しい低酸素状態となる．

染色した．このような虚血状態下のラット脳細動脈および周辺組織内の血中酸素分圧の空間分布を示したのが図 7 であり，梗塞した血管と周辺組織では著しい低酸素状態となる．図 7 は相対表示してあるが，梗塞した血管と周辺組織の酸素分圧は 10 mmHg 以下に低下してきわめて重篤な状態に陥る．これに対して正常状態下の血中酸素分圧は高く，組織中の酸素分圧は血管からの距離が隔たるに従って，一定の勾配をもって減少していく様子がわかる．図 3 に示したマウス背部皮膚腫瘍組織内の血流動態と酸素分圧も同様な方法で計測したが，腫瘍新生血管は管径が細く複雑な形態を示し，血管内皮が脆弱で血流速度は低く，酸素分圧もきわめて低い低酸素状態にある．相対的にみて正常な細静脈の酸素分圧は細動脈系の 50% 以下であり，また腫瘍新生血管では周辺組織で酸素消費が高いため，正常細静脈系よりさらに低い酸素状態にあることがわかった．

おわりに

血液循環の最大の目的は組織への酸素輸送である．組織とのガス交換を行う微小循環の計測は顕微鏡レベルの観測ゆえに技術的な困難さを伴い，今日まで多くの方法や装置が考案されてきたが，いまだ十分に要求に応えるものがないといっても過言ではない．本稿では，臓器微小循環における血流動態と酸素代謝を非接触・無侵襲で定量的に計測するための光・イメージング解析システムを紹介するとともに，蛍光・リン光プローブを用いて赤血球をはじめとする血液細胞の流動と，微小血管内および周辺組織内の酸素分圧を同時計測する方法について述べた．本システムは，脳，肝，腎などの実質臓器微小循環の血流ダイナミクスと，それによる酸素運搬能の定量化に有効であり，糖尿病，高血圧症，高脂血症などの病態における末梢循環障害，それに伴う酸素供給への影響の検討，また病態に対する薬理効果の評価，血液代替物の各種臓器微小循環における酸素運搬能の評価[5]，腫瘍新生血管の特異性評価，種々の病態モデルの生理機能や分子機構の解明などに大きな力を発揮すると考えられる．

文献

1) Minamitani, H. et al. : Imaging and functional analysis of blood flow in organic microcirculation. *J. Pharmacological. Sci.*, **93**(3) : 227-233, 2003.
2) Tsukada, K. et al. : Red blood cell velocity and oxygen tension measurement in cerebral microvessels by double-wavelength photoexcitation. *J. Applied Physiol.*, **96** : 1561-1568, 2004.
3) Minamitani, H. et al. : Measurement of blood flow and oxygen tension using fluorescent and phosphorescent probes in organ microcirculation. *Microcirculation Annual*, **18** : 13-14, 2002.
4) 南谷晴之・他：臓器血流と酸素代謝の光・イメージング解析，公開シンポジウム，ナノとバイオの融合学理構築，産業基盤形成．仙台，2003.
5) Tsukada, K. et al. : Blood flow analysis in cerebral microcirculation during exchange blood transfusion with hemoglobin-encapsulated liposome. *Microcirculation Annual*, **18** : 41-42, 2002.

ENHANCED PLATELET AGGREGABILITY IN DIABETIC PATIENT ESTABLISHED BY LASER LIGHT SCATTERING METHOD

Yasunori HIROSE[1], Eiichi SEKIZUKA[2], Chikara OSHIO[3], Taro IZUMIDA[2]
Hiromichi NAKADATE[1], Haruhiko GOKAN[1], Haruyuki MINAMITANI[1]

[1] Graduate School of Science and Technology Keio University
[2] Department of Clinical Research, National Saitama Hospital
[3] Oshio Clinic

INTRODUCTION

Diabetes mellitus (DM) is characteristic of chronic hyperglycemia, and causes various angiopathies. The population of diabetic patients continues to increase, so it is important to clear the mechanisms of angiopathies and to apply the resules for their treatments.

In previous study, we investigated the thrombus formation in the mesenteric arterioles of diabetic rats using a photochemical reaction. We confirmed that there was the shorting time of thrombus formation in diabetic rats. In this study, we focused enhanced platelet aggregability in DM and investigated the relationship between platelet aggregation and several physiological abnormalities in DM. We used laser-light scattering platelet aggregometer (PA-200, KOWA Company. Ltd., Tokyo, Japan) which is characterized by its high sensitivity to small platelet aggregation [1]. In order to appreciate the output data of PA-200, we used our original method to evaluate platelet aggrigability in early phase.

It has been said that fibrinogen is binding with activated platelet glycoprotein IIb/IIIa (GPIIb/IIIa) and its serum label increases in DM [2]. Additionally, it is said that blood concentration of fibrinogen is higher in DM [3]. Therefore, in the present study, we evaluated platelet aggregability by the method described above and compared the inhibitory effects of the GPIIb/IIIa antagonist on diabetic and healthy platelets. Furthermore, we evaluated the platelet aggregability that fibrinogen was added to platelet sample to investigate the relationship between increased fibrinogen and platelet aggregability in DM.

MATERIAL AND METHOD

The study group included six patients in low-grade DM (6.5%<HbA_{1c}<9%), six in high-grade DM (HbA_{1c}>9%), and seven healthy ones. Blood samples were collected into tubes containing 3.8% sodium citrate (9:1 v/v). Platelet rich plasma (PRP) was prepared by centrifugation at 150g for 10 min at room temperature. Platelet poor plasma (PPP) was prepared by centrifugation at 1500g for 15 min at room temperature. PRP was diluted by PPP and platelet concentration was adjusted to $3\times10^5/\mu l$.

To investigate the role of GPIIb/IIIa on enhanced platelet aggregability inDM, GPIIb/IIIa antagonist (FR144633, Fujisawa Pharmaceutical Co., Tokyo, Japan) was incubated for 30 min at 37°C to PRP (0.01, 0.1, 1.0 μM, final concentration). Similarly, to investigate about the relationship of fibrinogen on enhanced platelet aggrigability, human derived fibrinogen (Sigma Aldrich Japan K.K., Tokyo, Japan) was incubated for 30 min at 37°C to PRP (100, 200 mg/dl, final concentration). Dissolution of fibrinogen was confirmed by thrombin time method.

To measure platelet aggregability, first PRP 255 μl was put into cylindrical glass cuvette with a 5 mm diameter and PRP was stirred in 1000 rpm. He-Ne laser (675 nm, Toshiba, Tokyo, Japan) was pass through PRP. The light scattered from the observation volume (140×140×20 μm) was detected by a photodetector. Data were recorded as a twodimensional graph showing the change over time of total light intensity expressed as a cumulative summation at 10esond-intervals of scattered light intensity (Ii) and the number of particles corresponding to that intensity (Ni) in terms of particle size (intensity) (ΣIiNi)(volt×count per s). The total light intensities of small, medium and large aggregates were determined. Detected scattered light intensity is divided into the classes, small aggregates (9-25 μm), medium aggregates (25-50 μm) and large aggregates (50-70 μm), by the levels of light intensity.

Adenosine diphosphate (ADP, Sigma Aldrich Japan K.K., Tokyo, Japan) was added to PRP to induce platelet aggregation in 1 min after from starting measurement. The final concentration of ADP was 0.5 μM, which can induce slight platelet aggregation. To quantify platelet aggregability, integrated the value of the light intensity scattered from small-sized aggregates (9-25 μm, details are described above) for 2 min from the time of ADP induction. The reasons we adopt this method are to evaluate platelet aggregation in physiologic agonist concentration and thatthe enhanced platelet aggregation in early phase is characteristic in DM.

RESULT

LS correlated with HbA1c (r^2=0.37) and it means chronic hyperglycemia induced by DMresult to enhanced platelet aggregability. We comparedthe inhibiting effect of platelet aggregation by GPIIb/IIIa antibody (Fig. 1). Both in DM patient and healthy, GPIIb/IIIa antibody inhibited platelet aggregation wholly. Blood fibrinogen concentrationhad high correlation with HbA_{1c} (data not shown). Fibrinogen assumes a role as the adhesion molecule between platelet and platelet when platelets aggregate, so it was expected that theremight be the high correlation between

platelet aggregation and fibrinogen. But the correlation coefficient was low (r^2=0.34). Fig. 2 shows measurement result of platelet aggregability when fibrinogen was added to PRP. There were no significant difference among control group and fibrinogen-added groups.

DISCUSSION

We can present enhanced platelet aggregation in DMby our own method to evaluate a result measured by laser light scattering method. There are quite a lot of reports about enhanced platelet aggregability in DM. In DM, activation of arachidonic acid cascade in plaelets is accelerated, and it is believed to induce enhanced platelet aggregation. In platelet, activation of arachidonic acid cascade leads to greater formation of thromboxane A_2 (TXA_2). TXA_2 is a powerful agonist of platelet aggregation and, therefore, could contribute to the hypersensitivity of diabetic platelet. It was suggested that the aggregation in this measuring system is mediated by the binding between GPIIb/IIIa and fibrinogen. Combine with the result described above, platelet aggregability was increased in diabetes, it is suggested that fibrinogen binding increased in diabetic platelet. This result is consistent with Helen' s report, which investigates fibrinogen binding by ^{125}I-labeled fibrinogen [4].

In this study, there were the correlation between HbA_{1c} and fibrinogen (r^2=0.30). The correlation coefficient between fibrinogen and platelet aggregability was not high but not negligible. The results shown as Fig. 2, enhanced platelet aggregation were not observed when fibrinogen was added in platelet sample. Therefore it was suggested that increase of fibrinogen in DM doesn' t affect platelet aggregation. There are few studies argued about relationship between blood concentration of fibrinogen and platelet aggregation, but we could suggestthe increased fibrinogen does not directly influence platelet aggregability.

But the increase of fibrinogen considered enhancing clotting reaction. In diabetic retinopathy or neuropathy, fibrinogen and thrombin-antithrombin III complex increased significantly, and following abnormality of coagulation system is the contributing factor of these complexes.

CONCLUSION

We could measure precisely the enhanced platelet aggregability in DM by our own methodusing laser light scattering system. The increase of GPIIb/IIIa amounts or activities might contribute to the enhanced platelet aggregability in DM. Furthermore, from the result which platelet aggregation did not increase when fibrinogen was added to platelet samples, increase of fibrinogen in DM is not affect platelet aggregability.

REFERENCE

[1] Ozaki Y, Satoh K, Yatomi Y, Yamamoto T, Shirasawa Y, Kume S. Detection of platelet aggregations with a particle counting method counting method using light scattering. Anal Biochem. 1994; 218: 284-94

[2] Tschoepe D, Rosen P, Gries FA. Increase in the cytosolic concentration of calcium in platelets of diabetes type II. Thromb res. 1991; 62: 421-38

[3] Mansfield MW, Heywood DM, Grant PJ. Circulating levels of factor VII, fibrinogen, and von Willebrand factor and features of insulin resistance in first-degree relatives of patients with NIDDM. Circulation. 1996; 94: 2171-6.

[4] Leet H, Paton RC, Passa P, Caen JP. Fibrinogen binding and ADP-induced aggregation in platelets from diabetic subjects. Thromb Res. 1981; 24: 143-50

Key words: Diabetes mellitus, platelet aggregation, GPIIb/IIIa

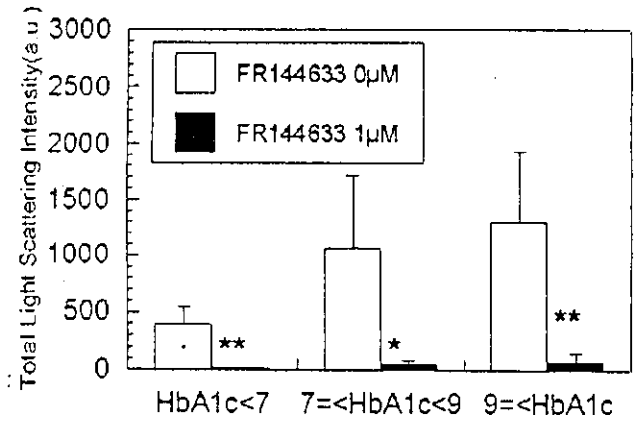

Fig. 1 Inhibition of platelet aggregation by GPIIb/IIIa antagonist. Aggregation was wholly inhibited by antagonist.
*p<0.05 vs 0μM, **p<0.01 vs 0μM

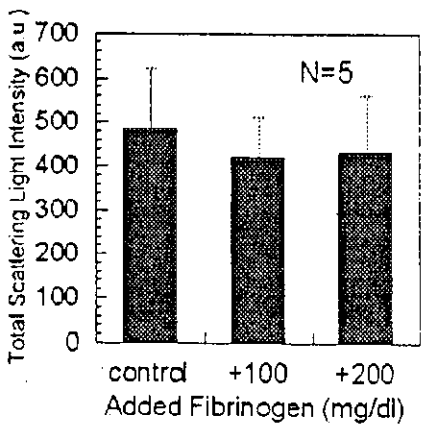

Fig. 2 Result of aggregability measurement when fibrinogen was added in platelet sample.
There were no significant differences among

The effect of shear stress on the accelerated adhesion of diabetic platelets

Hiromichi Nakadate[1], Eiichi Sekizuka[2], Chikara Oshio[3],
Yasunori Hirose[1], Haruhiko Gokan[1], Haruyuki Minamitani[1]

[1]Graduate School of Science and Technology, Keio University
[2]Department of Clinical Research, National Saitama Hospital
[3]Ryouyu-kai Medical corporation

Introduction

Diabetes mellitus has chronic hyperglycemia, and causes various vessel complications such as macroangiopathy and microangiopathy. Macroangiopathy includes major cardiovascular events and atherosclerosis, while microangiopathy is the characteristic affection of diabetes mellitus and contains retinopathy, neuropathy and nephropathy. In diabetes mellitus the high thrombogenesis is reported and thrombus formation is deeply concerned in these diabetic complications. But the mechanism of microangiopathy has not been demonstrated clearly.

Based on these backgrounds, we have been studying the mechanism in diabetic microangiopathy. First we suggested that high thrombogenesis was accelerated in diabetic microcirculation in rat mesentery. Moreover we focused on the interaction between platelets and vascular endothelial cells that played an important role of thrombus formation and carried out an *in-vitro* experiment. Additionally under no flow conditions we investigated the interaction between platelets and human umbilical vein endothelial cells (HUVECs) cultured in diabetic condition (high-glucose or high-AGE) in the model of photodynamic therapy (PDT) by using photopfrin. The endothelial cells contributed to the thrombus formation more strongly than platelets in diabetes mellitus. Under no flow without PDT, platelet adhesion to HUVECs increased much more in the diabetic conditions than in control one. In addition, we investigated the endothelial disorders by Reactive Oxidative Species (ROS).

But deeper appreciation of diabetic thrombogenesis requires the experimental condition like intravascular condition, which can make shear stress by flow.

Methods

We used flow chamber to investigated shear-induced platelet adhesion and aggregation on endothelial cells (Fig. 1). At first the blood of diabetic patient was flown over collagen-coated glass at high or low shear rate for 10 minutes. The blood' s platelets are stained by quinacrine and observed under fluorescence microscope. Platelet adhesion was estimated from the images taken by high-speed video camera. Moreover, we flew normal blood over HUVECs incubated in high glucose medium at high or low shear rate for 10 minutes and after washed, took the transfer images by the light microscope. Platelet adhesion was estimated by the images.

Results

Flown over collagen-coated glass, their platelets adhered more than normal platelets and the adhesion was more prominent at high shear rate than low shear rate (Fig. 2). Additionally, platelets adhered more to HUVECs incubated in high glucose medium than to normal HUVECs and the adhesion was more remarkable at high shear rate than low shear rate (Fig. 3). At present, the engagements of adhesion factors on platelet, endothelial cell, and in plasma, are additionally under consideration.

Conclusion

We recognized that platelet adhered to HUVECs under high shear stress in control condition, and in high glucose condition platelet adhesion to HUVECs increased according to high shear stress.

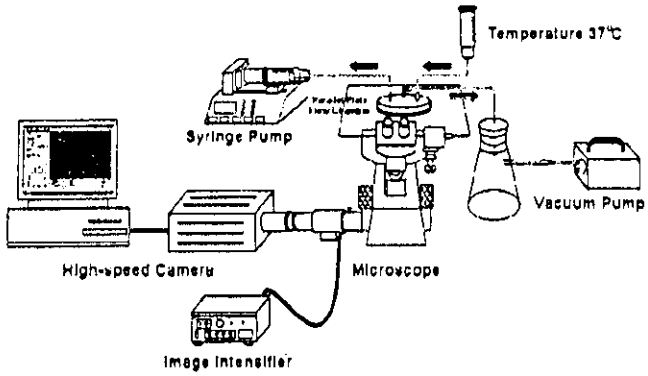

Fig. 1 Flow loading and recording system

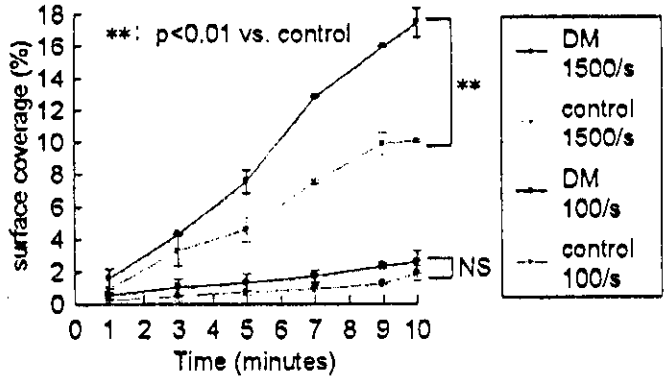

Fig. 2 Platelet adhesion on collagen at each shear rate (normal vs. diabetic)

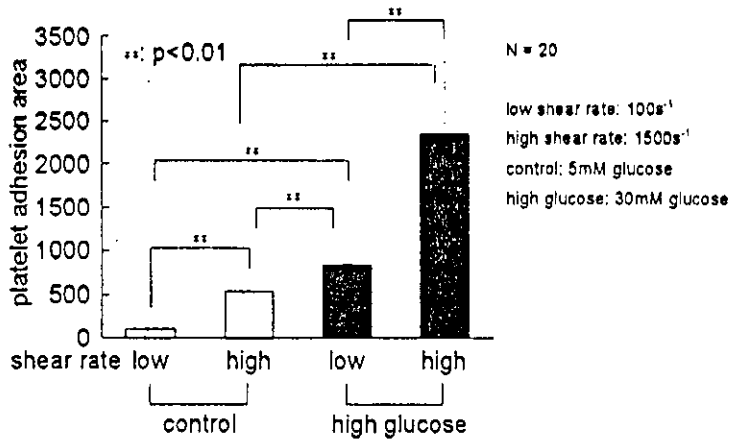

Fig. 3 Platelet adhesion area under each shear rate and glucose density

Key Words: diabetes mellitus, platelet adhesion, shear stress

Blood Flow Dynamics and Intravascular Oxygen Tension of Tumor Microvessels in Photodynamic Therapy

Noriko Shibuya[1], Yumiko Iwata[1], Akira Ushiyama[2], Haruyuki Minamitani[1], Chiyoji Ohkubo[2]
[1]Graduate School of Science and Technology, Keio University, [2]National Institute of Public Health

Formation of new blood vessels (angiogenesis) plays an important role in development, physiological repair processes, and various diseases such as the growth of solid tumors.

Photodynamic therapy (PDT) is accomplished by laser light excitation of photosensitizer accumulated in malignant tissues. This effect is thought to be not only direct tumor cell death, but also vascular stasis in tumor. PDT targeted to neovasculature may cause tumor regression through the deprivation of nutrient and oxygen in tumor tissues due to hemostasis. In recent studies, it is speculated that tumor necrosis depends on vascular shut down, rather than on direct tumor cell death. However, there are few reports on vascular shut down in tumor vessels and the mechanism which produce vascular shut down remains largely unknown. Furthermore, tumor blood flow is often sluggish and static, and even changes the direction over time. Resulting hypoxia and acidosis become hallmarks of tumors and critical determines of response to treatments. We developed in-vivo microscopy technique to simultaneously measure pO_2 and blood flow dynamics.

The experiments were performed in male BALB/C mice (6 to 8 weeks old, 25 to 30g). A dorsal skinfold chamber was implanted, and small peace of mouse mammary tumor was implanted (Fig.1).This study was designed to examine influence of photochemical reaction on blood flow dynamics of microcirculation using intravital microscopy with high speed video camera system and image analysis. For measurements of vessel diameter and red blood cell velocity, FITC-dx was injected into the tail vain for contrast enhancement between red blood cells and plasma. Red blood cells flow in the tissue microcirculation was recorded by using a high-speed video camera. The average values of the vessel diameter and wall shear rate in tumor vessels were found to be lower than those of the tumor free mice (Fig.2).Vascular shut down time in tumor vessels were shorter than that of the tumor free mice (Fig.3).

Oxygen tension pO_2 in arterioles, veins and tumor vessels were determined by oxygen-dependent quenching of phosphorescence technique. pO_2 was measured by phosphorescence quenching dependent on excitation of Pd-TCPP in the microvessel with the second harmonic of Nd:YAG pulse laser (532nm) and calculated from the Stern-Volmer equation (Fig.4). show. the difference of pO_2 in the microvessels. (Fig.5) shows profiles of pO_2 in mouse micro vessels and their surrounding interstitial spaces

The results indicate that in tumor vessels, vascular stasis is highly occurred by because of reduction of the vessel diameter and wall shear rate. Further more, tumor vessels have tortuous shape, and irregular intravascular surface that may provide the different oxygen profile. The technique in this study has allowed us to show the relationship between pO_2 and angiogenesis.

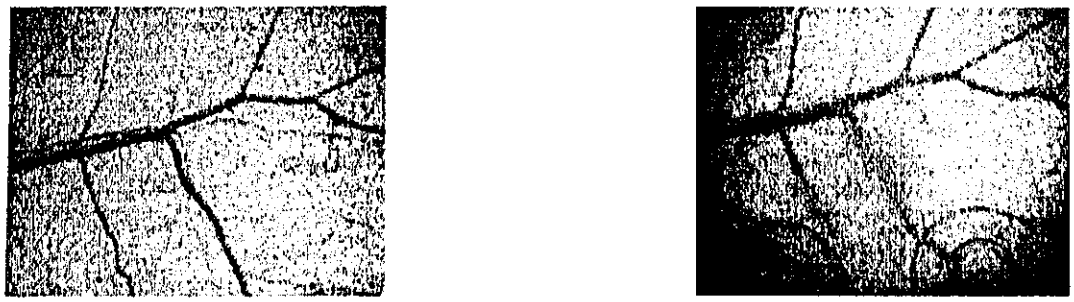

(a) Tumor-free (b) Tumor-bearing

Fig.1 microcirculation in mouse dorsal skinfold chamber

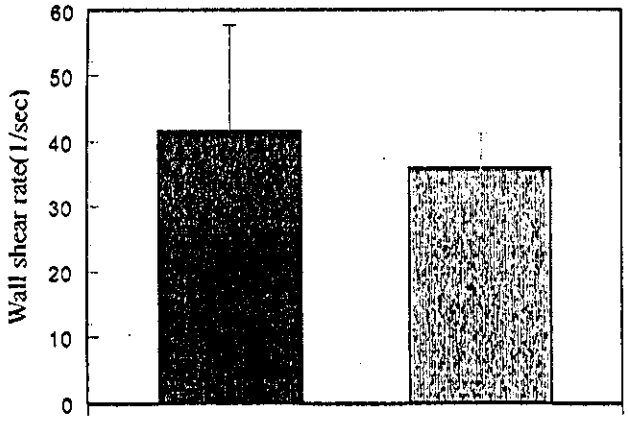

Fig.2 Wall shear rate in micro vessels of mouse dorsal skinfold chamber

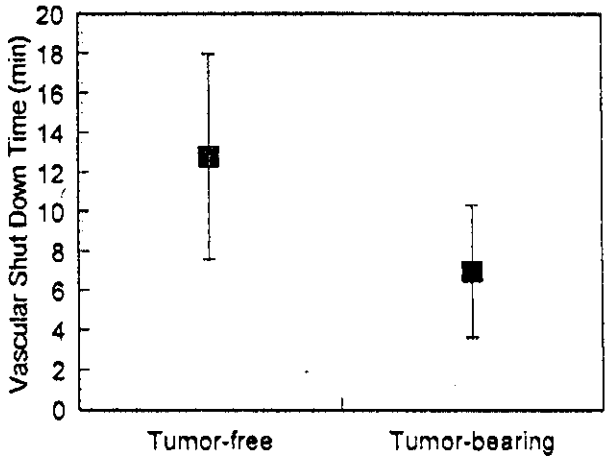

Fig.3 Vascular shut down time in micro vessels of mouse dorsal skinfold chamber

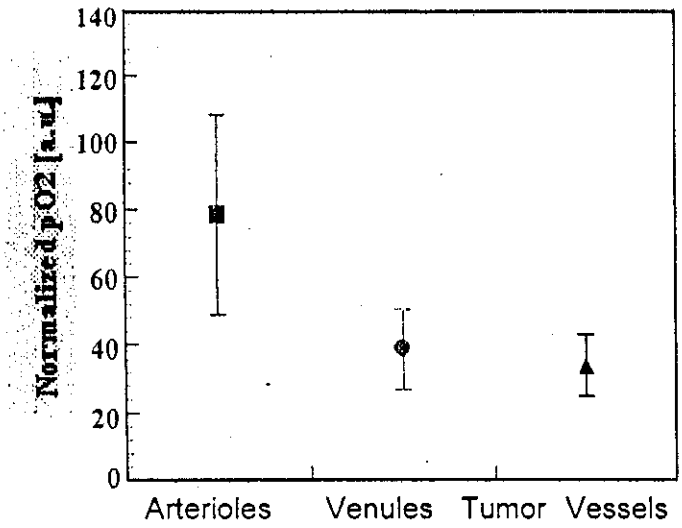

Fig.4 Oxygen tension pO_2 in mouse arterioles and veins and tumor vessels

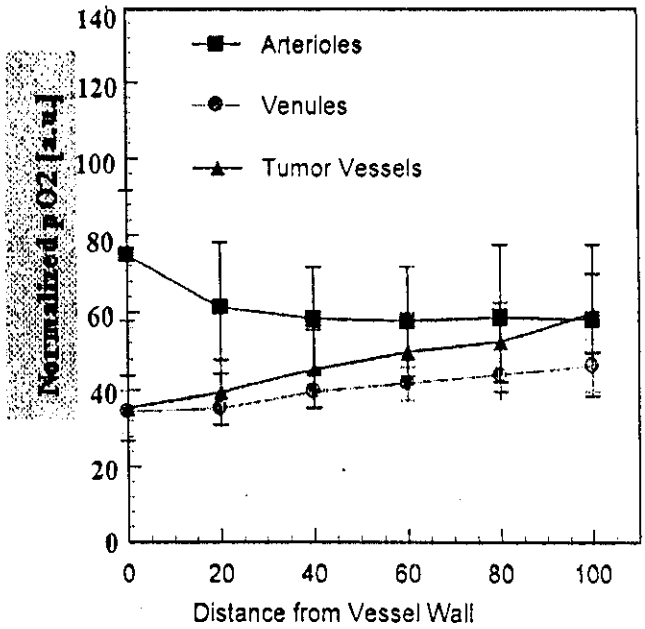

Fig.5 Profiles of pO_2 in mouse micro vessels and their surrounding interstitial spaces

Key Words: oxygen, tumor vessel, vascular stasis

Color imaging of platelets and leukocytes labeled with different fluorescent material in brain pial vessels of C57BL/6 mouse

Satoshi TERAO[1], Eiichi SEKIZUKA[2], Mami ISHIKAWA[5],
Noriyuki YAMAGUCHI[3], Haruyuki MINAMITANI[4], Takeshi KAWASE[5]
Department of [1]Neurosurgery and [2]Clinical Research, National Saitama Hospital, Saitama, Japan, [3]Department of Neurosurgery, Saitama Municipal Hospital, Saitama, Japan, [4]Institute of Biomedical Engineering, Faculty of Science and Technology, Keio University, Kanagawa, Japan, [5]Department of Neurosurgery, School of Medicine, Keio University, Tokyo, Japan

Introduction

Cranial window method can directly visualize the motion of blood cells in the brain pial vessels. And this method can be applied to small animals such as C57BL/6 mouse. But the problem was that platelets can be distinguished from leukocytes only from their size, because both of them are stained with same color (red), when using popular fluorescent agent, Rhodamine 6G. Color imaging of platelets and lekocytes labeled with different fluorescent materials is now tried through intravital microscope and 3CCD camera systems in the reperfusion injury model of the brain.

Materials and Methods

1) MCA occlusion and reperfusion model of C57BL/6 mice

C57BL/6 mice weighing 20-25g (6-7 weeks after birth) were anesthetized by intraperitoneal injection of alpha-chloralose (60mg/kg) and urethane (600mg/kg). Mice were tracheotomized and polyethylene tubes (PE-10) were cannulated into femoral artery and vein. Rectal temperature was maintained at 37℃ by heating lamp, and blood pressure was monitored continuously. 6-0 nylon thread was inserted into left internal carotid artery from external carotid arterial stump until its top reached approximately 9-10mm distal from the bifurcation of the common carotid artery. Middle cerebral artery (MCA) was occluded by this maneuver and the achievement of MCA occlusion (MCAO) was ensured by reduced cerebral blood flow (CBF) on the left parietal cortex of MCA territory measured by transcranial Laser Doppler flow meter (below 10% compared to the opposite side). After 1 hour occlusion, MCA was re-canalized by pulling out the nylon thread (MCAO/R).

2) Ex vivo preparation and staining of platelets

Other C57BL/6 mice were anesthetized in the same fashion as above. Whole blood was collected from left common carotid artery. Platelets were extracted by centrifugation and stained *ex vivo* with carboxyfluorescein diacetate succinimidyl ester (CFDASE). Finally platelets were suspended in PBS and the concentration of platelets was counted (μl^{-1}).

3) Color imaging of platelets and leukocytes

MCAO/R mice were fixed in sphinx position by the stereotaxic head frame. A small cranial window (approximately 3mm in diameter) was made on the left parietal bone (1mm posterior and 4mm lateral to the bregma). Dura mater was not incised.

After 4 hour reperfusion, 0.05% Rhodamine 6G was infused continuously. Platelets, prepared *ex vivo* and stained with CFDASE, were also injected simultaneously for few minutes. Total amount of injected platelets was 100×10^6/body. Using water immersion lens and double band filter, color image of the platelets and leukocytes rolling in the brain pial vessels was recorded through intravital microscope bearing 3CCD camera system.

Results

Leukocytes (stained into red with Rhodamine 6G) and platelets (stained into green with CFDASE) could be visualized as a dual-color image and easily distinguished from each other. They were rolling and sometimes adhered to each other.

Conclusions

Because the dura mater of mice is very thin, color CCD camera system can capture weak